An Unambiguous Radar Mode with a Single PRF Wideband Waveform

M. Lasserre, S. Bidon
ISAE / University of Toulouse,
Toulouse, France
Email: name.surname@isae.fr

F. Le Chevalier
MS^3,Delft University of Technology,
Delft, The Netherlands
Email: F.LeChevalier@tudelft.nl

***Abstract*—In this paper, we consider the problem of unambiguously estimating targets, including in blind velocities, using a single-low-PRF wideband radar signal. We present a Bayesian sparse recovery algorithm able to estimate the amplitude and location of range-migrating targets possibly straddling range-velocity bins embedded in colored noise. Numerical simulations on synthetic data and experimental data show that the proposed algorithm is able to mitigate velocity ambiguity and estimate targets in blind velocities.**

I. Introduction

Using conventional radars that transmit a train of pulses with constant pulse repetition frequency (PRF) leads to two types of ambiguities: range ambiguities (if the PRF is too high) or velocity ambiguities (if the PRF is too low) [1], [2]. Besides, the ambiguous range and ambiguous velocity are related such that their product only depends on the carrier frequency: increasing one will decrease the other. Wideband radars offer an alternative to the problem of ambiguity removal: as range resolution is increased, fast moving targets are likely to migrate during the coherent processing interval (CPI) leading to range-velocity coupling [3], [4]. Assuming that a low PRF is used, many velocity ambiguities appear; however, the above-mentioned "range walk phenomenon" gives additional information that can be used to obtain unambiguous velocity measurement [4].

Sparse signal representations (SSR) can be of particular interest when trying to remove velocity ambiguities since they allow the estimation of a sidelobe-less signal of interest (SOI) [5], [6]. In [7], SSR is used to obtain unambiguous estimation of fast moving targets. More precisely, a hierarchical Bayesian approach is adopted and sparsity is enforced on the target amplitude vector via a mixed-type prior distribution. Yet, the algorithm from [7] is limited to the case of targets whose features match that of the analysis grid used to discretize the range-velocity domain ("on-grid" targets, as opposed to "off-grid" targets); they are also embedded in white noise. However, as experimental radar scenes often contain off-grid targets and/or colored noise, this algorithm needs to be robustified with respect to (wrt) these two phenomena to prevent false-estimations in the clutter and targets' sidelobes and hence mitigate velocity ambiguities. This work focuses on the robustification of the algorithm from [7] towards these two phenomena using the sampling scheme modifications described in [8] and [9]. In [8], robustification towards grid mismatch is investigated. The mismatch between the target's features and the analysis grid is modeled by two vectors, called "mismatch vectors", that are also estimated by the Bayesian algorithm. Hence, migrating targets potentially *off-grid* and embedded in white noise are unambiguously estimated. In [9], the colored noise case is studied: an auto-regressive (AR) noise model is adopted and its parameters are estimated. Thus, "on-grid" migrating targets embedded in *colored noise* are discriminated from their ghosts and from the clutter sidelobes.

In this paper, we present a new algorithm robust to both grid-mismatch *and* colored noise using the hypothesis presented in [8] and [9] resp. *The technical novelty consists in merging two branches of the hierarchical Bayesian schemes presented separately in [8] and [9].* This modification affects non-trivially the sampling scheme, especially that of the mismatch vectors. The new algorithm is able to mitigate velocity ambiguity and estimate targets hidden in the clutter sidelobes for both synthetic and experimental data.

In Section II, the wideband signal model and SSR formulation are recalled. In Sections III and IV the hierarchical Bayesian model and estimation scheme adopted are presented. The proposed algorithm is then evaluated via numerical simulations on synthetic and semiexperimental data in Section V.

II. Signal model

We consider a wideband radar system sending M pulses with PRF f_r, meaning that the wideband B is non-negligible compared with the carrier frequency f_c. Processing of the data is done on a low-range resolution (LRR) segment consisting of K adjacent range bins. After applying a range transform, one can say that the samples are expressed in the fast-frequency/slow-time domain by a $K \times M$ data matrix $\boldsymbol{Y}$ [7], whose row-vectorized version denoted $\boldsymbol{y}$ is expressed as

$$\boldsymbol{y} = \sum_{n=1}^{N} \alpha_n \boldsymbol{a}_n + \boldsymbol{n} \tag{1}$$

The signature of the nth target is the product of a conventional 2D-cisoid and a cross-coupling term modeling range migration

$$[\boldsymbol{a}_n]_{m+kM} = \exp\left\{-j2\pi\left(\tau_0 \frac{B}{K} k - \frac{2v f_c}{c f_r}\left(1+\mu k\right) m\right)\right\} \tag{2}$$

The work of M. Lasserre is supported by the Direction Générale de l'Armement under grant 2014.60.0045 ISAE 2014-CIF-R90.

where τ_0 is the initial round-trip delay of the nth scatterer, $(2vf_c)/(cf_r)$ is the usual normalized Doppler frequency. In the following we use the fractional bandwidth per subband $\mu = B/(Kf_c)$.

A. SSR formulation

Following the approach used in [7], [8], the received signal $\boldsymbol{y}$ is reformulated within the scope of SSR as

$$\boldsymbol{y} = \boldsymbol{H}\boldsymbol{x} + \boldsymbol{n} \tag{3}$$

where $\boldsymbol{H}$ is a sparsifying dictionary that stems from a discretization of the range-velocity dimensions ($\bar{K}\bar{M}$ being the dimensions of reconstruction of the scene) and $\boldsymbol{x}$ is a sparse vector representing the target amplitude. Then, using (2) the $\bar{i}$th column of the dictionary $\boldsymbol{H}$ is expressed as

$$[\boldsymbol{h}_{\bar{i}}]_i = \frac{1}{\sqrt{KM}} \exp\left\{j2\pi\left(-f_{r\bar{i}}k + f_{d\bar{i}}(1+\mu k)m\right)\right\} \tag{4}$$

where $f_{r\bar{i}}$ and $f_{d\bar{i}}$ are the normalized range and Doppler frequencies from the range and velocity analysis grids. The table indices k, m, i and $\bar{k}$, $\bar{m}$, $\bar{i}$ used to index the sparsifying dictionary $\boldsymbol{H}$ are related as $i = m + kM$ ($k \in \{0, K-1\}$, $m \in \{0, M-1\}$) and similarly for $\bar{i}$, $\bar{k}$, $\bar{m}$.

B. Grid-mismatch modeling

As presented in [8], the range and velocity analysis grid are divided into $\bar{K}$ (resp. $\bar{M}$) bins with a possible zero-padding factor denoted n_{zp}^r (resp. n_{zp}^v) and an unfolding factor n_{va} on the velocity axis in order to mitigate velocity ambiguity. The number of range and velocity analysis bins are then $\bar{K} = n_{zp}^r K$ and $\bar{M} = n_{zp}^v n_{va} M$ resp. Besides, two mismatch vectors $(\boldsymbol{\varepsilon}^v, \boldsymbol{\varepsilon}^r)$ are introduced to address the mismatch problem on the velocity and range axis resp. and directly parametrize the sparsifying dictionary $\boldsymbol{H}$ [8]. Hence, a target located at the $\bar{i}$th analysis bin is characterized by its normalized Doppler frequency $f_{d\bar{i}}$ and normalized range frequency $f_{r\bar{i}}$

$$f_{d\bar{i}} = \frac{\bar{m}' + \varepsilon_{\bar{i}}^v}{\bar{M}} n_{va}, \qquad f_{r\bar{i}} = \frac{\bar{k} + \varepsilon_{\bar{i}}^r}{\bar{K}}. \tag{5}$$

where (assuming $\bar{M}$ is even) $\bar{m}' = \bar{m}$ if $\bar{m} \in \{0, ..., \bar{M}/2-1\}$; $\bar{m}' = \bar{m} - \bar{M}$ if $\bar{m} \in \{\bar{M}/2, ..., \bar{M}-1\}$.

C. Noise modeling

Using the method of [9], the following assumptions are made on the noise vector $\boldsymbol{n}$ 1) it models both thermal noise and clutter and is centred Gaussian: $\boldsymbol{n} \sim \mathcal{CN}(\boldsymbol{0}, \boldsymbol{R})$; 2) it is decorrelated from subband to subband; 3) it is correlated in the slow-time according to a stationary auto-regressive (AR) process with finite order P; 4) the clutter is locally homogeneous (i.e., the AR coefficients are subband-independent). These assumptions imply that the $KM \times KM$ covariance matrix $\boldsymbol{R}$ has the following structure

$$\boldsymbol{R} = \boldsymbol{I}_K \otimes \boldsymbol{\Gamma} \tag{6a}$$

$$\boldsymbol{\Gamma}^{-1} = \sigma_{\text{AR}}^{-2}(\boldsymbol{I}_M - \boldsymbol{\Phi})^H(\boldsymbol{I}_M - \boldsymbol{\Phi}) \tag{6b}$$

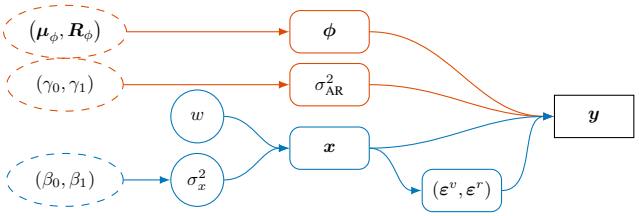

Fig. 1. Directed acyclic graph associated with the proposed hierarchical Bayesian model. The upper part of the model (orange) corresponds to the noise modeling proposed in [9] while the bottom part (blue) corresponds to the target amplitude and grid mismatch modeling of [8].

where $\boldsymbol{\Gamma}^{-1}$ is a P-banded $M \times M$ matrix; its Cholesky factorization is given by (6b) where $\boldsymbol{\Phi}$ is a lower-triangular Toeplitz matrix with zero diagonal elements that gives the AR coefficients: $\boldsymbol{\Phi} = \text{Toeplitz}\left\{\begin{bmatrix}0 & \phi_1 & \dots & \phi_P & 0 & \dots & 0\end{bmatrix}\right\}$; σ_{AR}^2 is the variance of the white input to the AR model.

Hence, the likelihood function is given by

$$f\left(\boldsymbol{y}|\boldsymbol{\varepsilon}^v, \boldsymbol{\varepsilon}^r, \boldsymbol{x}, \boldsymbol{R}\right) = \frac{e^{-(\boldsymbol{y}-\boldsymbol{H}(\boldsymbol{\varepsilon}^v,\boldsymbol{\varepsilon}^r)\boldsymbol{x})^H \boldsymbol{R}^{-1}(\boldsymbol{y}-\boldsymbol{H}(\boldsymbol{\varepsilon}^v,\boldsymbol{\varepsilon}^r)\boldsymbol{x})}}{\pi^{KM}|\boldsymbol{R}|}$$
$$= \frac{\exp\left\{-\sigma_{\text{AR}}^{-2}||\left[\boldsymbol{I}_K \otimes (\boldsymbol{I}_M - \boldsymbol{\Phi})\right](\boldsymbol{y} - \boldsymbol{H}(\boldsymbol{\varepsilon}^v, \boldsymbol{\varepsilon}^r)\boldsymbol{x})||^2\right\}}{\pi^{KM}\sigma_{\text{AR}}^{2\ KM}} \tag{7}$$

Note that $||\cdot||$ designates the ℓ_2-norm $\|\cdot\|_2$ throughout the document.

III. Bayesian model

A hierarchical Bayesian model is used to estimate the parameters of interest, namely $\boldsymbol{x}, (\boldsymbol{\varepsilon}^v, \boldsymbol{\varepsilon}^r)$; it is graphically represented in Fig. 1. The unknown parameters are considered as random variables and a prior distribution is assigned to each of them; these prior pdfs are briefly detailed hereafter since they are the ones presented in [8], [9].

A. Target amplitude vector $\boldsymbol{x}$

The elements of the target amplitude vector $\boldsymbol{x}$ are considered iid a priori; they are distributed according to the following mixed-type pdf

$$\pi(x_{\bar{i}}|w, \sigma_x^2) = (1-w)\delta(|x_{\bar{i}}|) + w\frac{1}{\pi\sigma_x^2}\exp\left\{-\frac{|x_{\bar{i}}|^2}{\sigma_x^2}\right\}. \tag{8}$$

This prior, denoted $\mathcal{BerCN}\left(w, 0, \sigma_x^2\right)$, decorrelates sparsity level and target power via its mixed-type structure.

B. Mismatch vectors $(\boldsymbol{\varepsilon}^v, \boldsymbol{\varepsilon}^r)$

The elements of $(\boldsymbol{\varepsilon}^v, \boldsymbol{\varepsilon}^r)$ are supposed iid and conditioned by the corresponding value of target amplitude

$$\pi(\varepsilon_{\bar{i}}^v, \varepsilon_{\bar{i}}^r|x_{\bar{i}} = 0) = \delta(\varepsilon_{\bar{i}}^v)\delta(\varepsilon_{\bar{i}}^r) \tag{9a}$$

$$\pi(\varepsilon_{\bar{i}}^v, \varepsilon_{\bar{i}}^r|x_{\bar{i}} \neq 0) = \mathbb{I}_{[-0.5,0.5]^2}(\varepsilon_{\bar{i}}^v, \varepsilon_{\bar{i}}^r) \tag{9b}$$

where $\mathbb{I}_{[-0.5,0.5]^2}(\varepsilon_{\bar{i}}^v, \varepsilon_{\bar{i}}^r)$ is the indicator function of the set $[-0.5, 0.5] \times [-0.5, 0.5]$.

C. Disturbance parameters σ^2_{AR}, $\boldsymbol{\phi}$

The prior distributions assigned to the disturbance parameters σ^2_{AR}, $\boldsymbol{\phi}$ are that of [9]: conjugate priors are chosen, namely an inverse-gamma prior for σ^2_{AR} and complex-Gaussian prior for $\boldsymbol{\phi}$

$$\sigma^2_{\text{AR}}|\gamma_0,\gamma_1 \sim \mathcal{IG}\left(\gamma_0,\gamma_1\right) \tag{10a}$$

$$\boldsymbol{\phi}|\boldsymbol{\mu}_\phi,\boldsymbol{R}_\phi \sim \mathcal{CN}_P\left(\boldsymbol{\mu}_\phi,\boldsymbol{R}_\phi\right) \tag{10b}$$

where (γ_0,γ_1) are the shape and scale parameters of (10a) and $(\boldsymbol{\mu}_\phi,\boldsymbol{R}_\phi)$ are the a priori mean vector and covariance matrix of $\boldsymbol{\phi}$. In practice, both priors are adjusted to flat non-informative distributions since prior knowledge about the disturbance parameters may not be available:

$$\pi(\sigma^2_{\text{AR}}) \propto \frac{1}{\sigma^2_{\text{AR}}}\mathbb{I}_{[0,+\infty)}(\sigma^2_{\text{AR}}) \tag{11a}$$

$$\pi(\boldsymbol{\phi}) \propto 1. \tag{11b}$$

D. Hyperparameters σ^2_x and w

The hyperparameters of (8) are unknown so a final stage is added to the hierarchical Bayesian model. Following the approach used in [7], an inverse-Gamma prior is assigned to the target power σ^2_x and a uniform prior to the level of occupancy w

$$\sigma^2_x|\beta_0,\beta_1 \sim \mathcal{IG}\left(\beta_0,\beta_1\right) \tag{12}$$

$$w \sim \mathcal{U}_{[0,1]}. \tag{13}$$

IV. Bayesian estimation scheme

As mentioned in Section III, the target scene is estimated via the parameters of interest $\boldsymbol{x},(\boldsymbol{\varepsilon}^v,\boldsymbol{\varepsilon}^r)$ by deriving Bayesian estimation based on the hierarchical model described in Fig. 1. More precisely, the MMSE estimators of $\boldsymbol{x}$ and $(\boldsymbol{\varepsilon}^v,\boldsymbol{\varepsilon}^r)$ are calculated

$$\hat{\boldsymbol{x}}_{\text{MMSE}}=\int \boldsymbol{x} f(\boldsymbol{x}|\boldsymbol{y})d\boldsymbol{x}, \tag{14a}$$

$$\left(\hat{\boldsymbol{\varepsilon}^v},\hat{\boldsymbol{\varepsilon}^r}\right)_{\text{MMSE}}=\int \left(\boldsymbol{\varepsilon}^v,\boldsymbol{\varepsilon}^r\right) f(\boldsymbol{\varepsilon}^v,\boldsymbol{\varepsilon}^r|\boldsymbol{y})d\boldsymbol{\varepsilon}^v d\boldsymbol{\varepsilon}^r. \tag{14b}$$

As (14) seems intractable to derive analytically, a Monte-Carlo Markov Chain (MCMC) algorithm is used. Compared to the sampling schemes of [8] and [9], several iterative steps are highly impacted by the mismatch and colored noise hypothesis. First, compared to the sampling scheme under white noise hypothesis of [8], the sampling of the target amplitude vector $\boldsymbol{x}$ and that of the variance of the white noise input σ^2_{AR} must take into account the whitened version of parameters $\boldsymbol{y}$ and $\boldsymbol{H}$, i.e., $\tilde{\boldsymbol{y}} \triangleq [\boldsymbol{I}_K \otimes (\boldsymbol{I}_M - \boldsymbol{\Phi})]\,\boldsymbol{y}$ and $\tilde{\boldsymbol{H}} \triangleq [\boldsymbol{I}_K \otimes (\boldsymbol{I}_M - \boldsymbol{\Phi})]\,\boldsymbol{H}$. Most importantly, the sampling of the mismatch vectors $(\boldsymbol{\varepsilon}^v,\boldsymbol{\varepsilon}^r)$ is a very demanding task wrt the white noise case of [8]. More precisely, the joint-sampling of $(\boldsymbol{\varepsilon}^v,\boldsymbol{\varepsilon}^r)$ must take into account the cross-coupling terms (due to migration) and unfolding factor (for velocity disambiguation) of the sparsifying dictionary $\boldsymbol{H}$, as well as the AR noise model.

V. Numerical simulations

A. Synthetic data

First, synthetic data is generated using (1), (2) and (6) with $P = 1$. Each target is characterized by its *post-processing* signal-to-interference-plus-noise ratio (SINR) calculated as

$$\text{SINR} = \mathcal{E}\left\{|\alpha|^2\right\}\boldsymbol{a}^H\boldsymbol{R}^{-1}\boldsymbol{a}. \tag{15}$$

Fig. 2 shows a target map estimated by the proposed algorithm robustified towards grid mismatch and using an AR noise model ("AR+mismatch algorithm") and by the different unrobustified and partially robutified versions of the algorithm: "AR + no mismatch", "WN + mismatch" (white noise model), "WN + no mismatch". One can see in Fig. 2(a) that the algorithm unrobustified towards grid mismatch and under white noise hypothesis leads to many false-alarms in the clutter sidelobes and that target 3 and 4 are split on the surrounding range bins. When robustified towards grid mismatch, the algorithm does not split targets 3 and 4 anymore but the numerous false alarms in the clutter sidelobes remain and target 2 is hidden amongst these (Fig. 2(b)). On the other hand, using an AR noise model without robustification towards grid mismatch does remove the false-alarms in the clutter sidelobes but targets 3 and 4 are split on both the range and velocity sidelodes (Fig. 2(c)). Finally, one can see in Fig. 2(d) that the four targets are accurately estimated by the AR+mismatch algorithm. Fig. 2(e) and 2(f) depicts the spectrum resulting from the AR parameters estimated by the AR+no mismatch and AR+mismatch algorithms resp. They show good agreement with the true one, verifying that the whitening operation required within the sampler is well achieved.

B. Experimental data

The AR+mismatch algorithm is then tested on semiexperimental data consisting in synthetic targets added to experimental clutter recorded by the PARSAX radar from Delft University of Technology (TU Delft) [10]. As in the synthetic case, one can see in Fig. 3(d) that the AR+mismatch algorithm does mitigate velocity ambiguities while the unrobustified and partially robustified versions of the algorithm lead to false alarms in the blind velocities (Fig. 3(a) and 3(e)) and/or split targets (Fig. 3(a), 3(b), 3(c)). Interestingly, one can see in Fig. 3(f) that the proposed algorithm interprets PARSAX clutter as the sum of a diffuse component and discretes, which was already observed in [9].

VI. Conclusion

In this paper, a Bayesian sparse recovery algorithm able to mitigate velocity ambiguities has been presented. It estimates the unambiguous location and amplitude of possibly off-grid migrating targets embedded in colored noise, even when located in the blind velocities. More precisely, an AR noise model has been adopted and associated with a robustified sparsifying dictionary; the parameters of interest are then estimated thanks to a Monte-Carlo Markov chain algorithm.

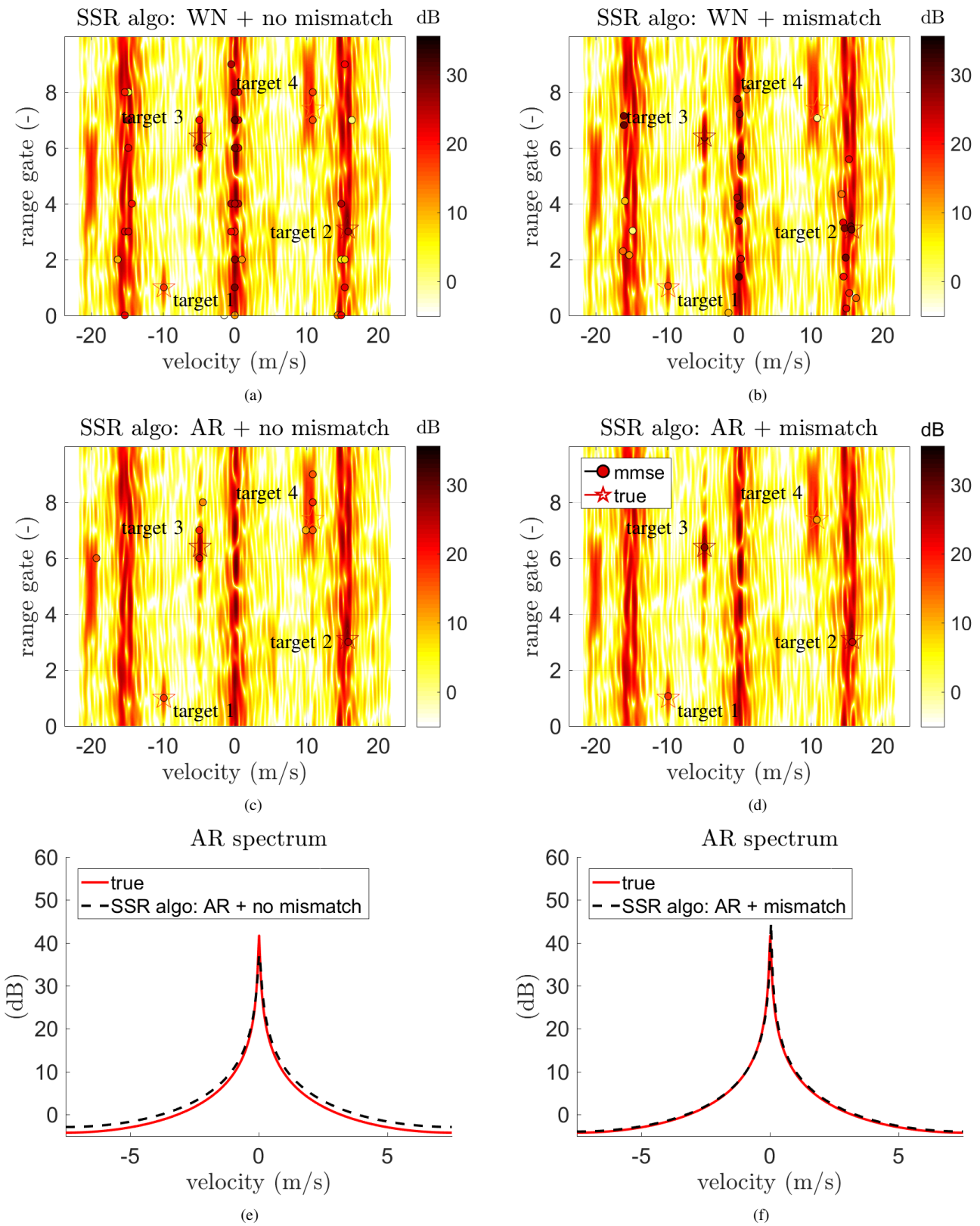

Fig. 2. Synthetic data processed by the proposed AR+mismatch algorithm (2(d), 2(f)), the unrobustified (WN+no mismatch, 2(a)) and partially robustified versions: WN+mismatch (2(b)), AR+no mismatch (2(c),2(e)); the scenario consists in 3 exo and one endo-clutter targets with SINR values 20, 15, 30 and 15 dB resp. (target 1 to 4). Coherent integration of the scene is represented in the background. $K = 10$, $M = 32$, $f_c = 10$ GHz, $B = 1$ GHz, $v_a = 15$ m/s. Synthetic AR: $\sigma^2_{\text{AR}} = 1.5$, $\phi = .99$. $\bar{K} = K$, $n_{va} = 3$, $\bar{M} = 3M$, $(m_{\sigma^2_x}, std_{\sigma^2_x}) = (35, 10)$ dB, flat prior on σ^2_{AR}.

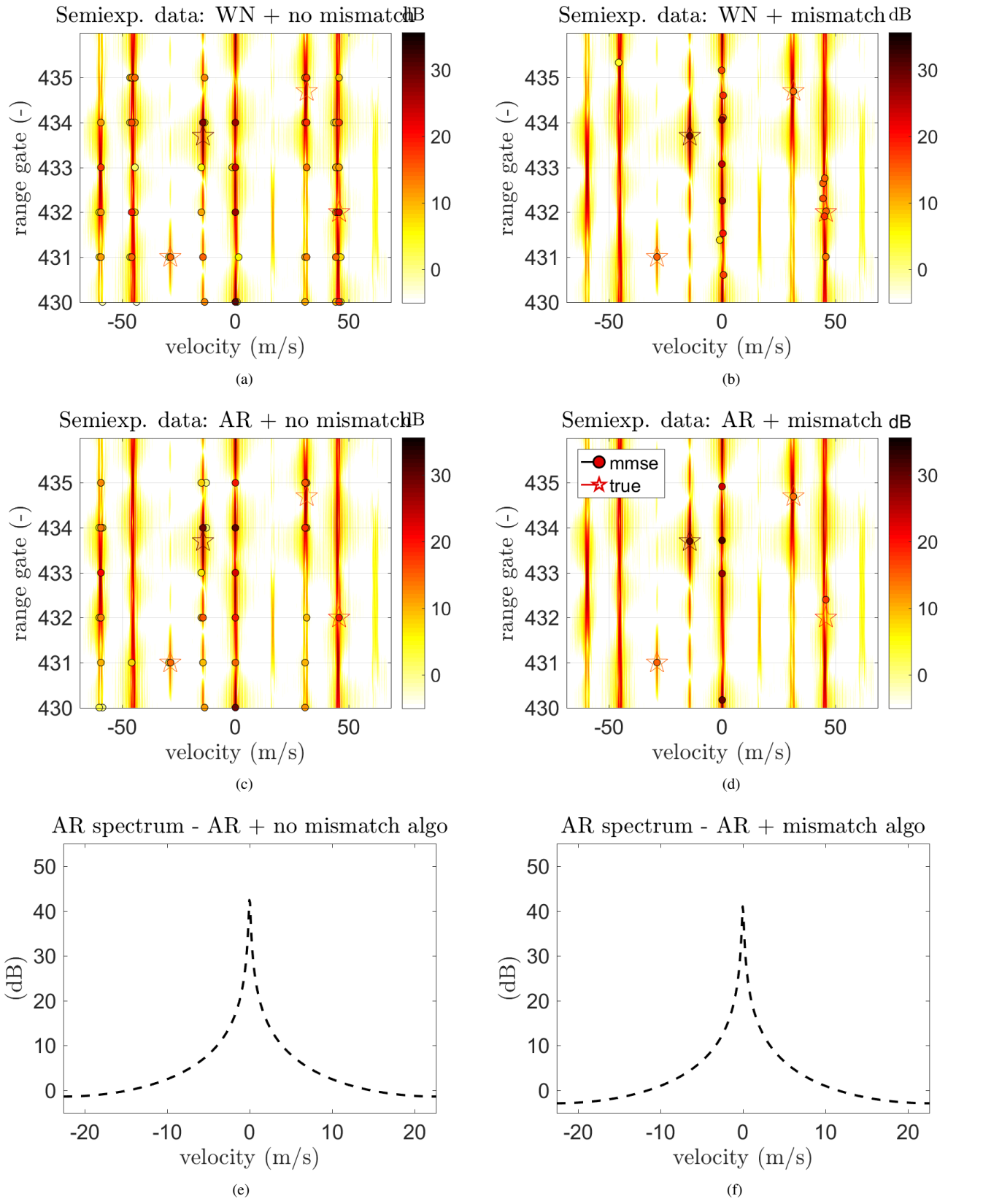

Fig. 3. Semiexperimental PARSAX data processed by the proposed AR+mismatch algorithm (3(d), 3(f)), the unrobustified (WN+no mismatch, 3(a)) and partially robustified versions: WN+mismatch (3(b)), AR+no mismatch (3(c),3(e)); the scenario consists in 3 exo and one endo-clutter targets with SINR values 15, 20, 30 and 15 dB resp. (target 1 to 4). Coherent integration of the scene is represented in the background. $K = 6$, $M = 64$, $f_c = 3.315$ GHz, $B = 100$ MHz, $v_a = 45$ m/s. $\bar{K} = K$, $n_{va} = 3$, $\bar{M} = 3M$, $(m_{\sigma_x^2}, std_{\sigma_x^2}) = (30, 10)$ dB, flat prior on σ^2_{AR}.

The proposed algorithm is successfully evaluated on synthetic and experimental radar data: velocity ambiguities are mitigated and the diffuse clutter component is assimilated by the AR model. In the future, a detection scheme has yet to be determined using the full Bayesian model and estimation technique presented here.

ACKNOWLEDGEMENT

The authors would like to thank O. Krasnov at TU Delft for kindly providing the PARSAX experimental data.

REFERENCES

[1] M. Richards, *Fundamentals of Radar Signal Processing*. McGraw-Hill Electronic Engineering, 2005.

[2] M. Skolnik, *Radar Handbook*. New York: McGraw-Hill, 1990.

[3] W. Melvin and J. Scheer, Eds., *Principles of Modern Radar: Advanced Techniques*. Edison, NJ: Institution of Engineering and Technology, 2012.

[4] F. Le Chevalier, *Principles of Radar and Sonar Signal Processing*. Artech House, 2002.

[5] J. Tsao and B. D. Steinberg, "Reduction of sidelobe and speckle artifacts in microwave imaging: the CLEAN technique." *IEEE Trans. Antennas Propag.*, vol. 36, no. 4, pp. 543–557, 1988.

[6] G. Davis, "Adaptive greedy approximations," *Constructive Approximation*, vol. 13, pp. 57–98, 1997.

[7] S. Bidon, J.-Y. Tourneret, L. Savy, and F. Le Chevalier, "Bayesian sparse estimation of migrating targets for wideband radar," *IEEE Trans. Aerosp. Electron. Syst.*, vol. 50, no. 2, pp. 871–886, Apr. 2014.

[8] M. Lasserre, S. Bidon, and F. L. Chevalier, "Velocity ambiguity mitigation of off-grid range migrating targets via bayesian sparse recovery," in *2016 IEEE Statistical Signal Processing Workshop (SSP)*, June 2016, pp. 1–5.

[9] S. Bidon, O. Besson, J.-Y. Tourneret, and F. Le Chevalier, "Bayesian Sparse Estimation of Migrating Targets in Autoregressive Noise for Wideband Radar," in *Proc. of IEEE International Radar Conference*, Cincinnati,OH, May 2014.

[10] O. A. Krasnov, G. P. Babur, Z. Wang, L. P. Ligthart, and F. van der Zwan, "Basics and first experiments demonstrating isolation improvements in the agile polarimetric FM-CW radar – PARSAX," *International Journal of Microwave and Wireless Technologies*, vol. 2, pp. 419–428, 8 2010.